PHYSICAL REVIEW A VOLUME 16, NUMBER 3 SEPTEMBER 1977

Experimental study of the propagation of ion acoustic solitons in a warm multi-ion plasma

M. Q. Tran and Ch. Hollenstein
Centre de Recherche en Physique des Plasmas, Ecole Polytechnique Fédérale de Lausanne, CH-1007 Lausanne, Switzerland
(Received 22 October 1976)

The formation of ion acoustic solitons in an argon-helium plasma is studied as a function of the light-ion concentration. It is found that an initial perturbation does not break into solitons for $1\% \lesssim \alpha \lesssim 66\%$. This fact can be related to an increase in linear Landau damping and to nonlinear resonant particles, i.e., reflected ions in front of the potential hump and eventually trapped ions between two solitons. In the concentration range where solitons are formed (essentially for $\alpha \gtrsim 66\%$) the soliton's Mach number and width follow qualitatively the well-known theoretical dependence on amplitude. Detailed studies show, however, that the measured Mach number cannot be explained by fluid theories (namely the Korteweg–de Vries equation and Sakanaka's theory). Stationary solutions from theory which takes into account trapped electrons and reflected ions adequately describe the Mach number versus amplitude and light-ion concentration dependence.

I. INTRODUCTION

Ion acoustic solitons excited in an argon plasma[1-3] are very sensitive to light-ion contamination. Ikezi[2] reported that in the presence of light ions outgassed from the vacuum vessel walls, the wave does not break into solitons but some turbulence is generated. In a previous experiment,[3] we also found that a high base pressure prevented soliton formation; however, we did not observe any turbulence. These experimental observations therefore suggest the necessity of a more precise study of the influence of a second ion species in the formation and propagation of ion acoustic solitons.

The effect of light-ion species has been investigated theoretically by White *et al.*[4] In the framework of fluid equations, they found that for small light-ion concentration α (defined as the ratio of light-ion density to total ion density), a soliton exists only if its amplitude is low enough not to reflect the light ions. For this case, a Korteweg–de Vries (K-dV) equation has been derived by Tran and Hirt[5] for ion temperature $T_i = 0$ and by Tran[6] for $T_i \neq 0$. The major result of this study is to show that light ions in a heavy-ion plasma drastically reduce the soliton amplitude for a given Mach number. Similar results have been obtained by Maxon[7] for cylindrical solitons.

Aside from these hydrodynamic effects, kinetic effects are very likely to occur. Usually in a pure plasma with high enough T_e/T_i, wave-particle interactions such as electron-ion Landau damping or trapping contribute as a small correction to the K-dV equation as has been shown by several authors.[8-10] Using the correct power ordering, van Dam and Taniuti[10] proved that the relevant smallness parameter ϵ for the ordering is given by $\epsilon \simeq (m_e/M_i)^{1/2}$ and not the disturbance amplitude. The domain of applicability of their theory is restricted to plasma parameters satisfying

$$\left.\frac{\partial f_{0i}}{\partial v}\right|_{v=\omega/k} = \frac{M_i}{m_e}\left.\frac{\partial f_{0e}}{\partial v}\right|_{v=\omega/k}. \tag{1}$$

Experimentally this ordering is no longer valid when a small number of light ions are added to a heavy-ion plasma. It has been shown both theoretically[11] and experimentally[12] that for small α, ω/k does not vary. For an Ar-He plasma, we have, therefore, the following ordering:

$$\left.\frac{\partial f_{0\mathrm{Ar}}}{\partial v}\right|_{v=\omega/k} \approx \epsilon,$$

$$\left.\frac{\partial f_{0\mathrm{He}}}{\partial v}\right|_{v=\omega/k} \approx 1.$$

One would therefore expect non-negligible kinetic effects. Whether kinetic or hydrodynamic effects will dominate is a question which can be solved only experimentally, since, to our knowledge, no theory has been developed for the case where the ordering $\delta f_0/\delta v \sim (m_e/M_i)^{1/2}$ is no longer valid.

In Sec. II the experimental apparatus will be described. The propagation of a nonlinear compressional pulse in an argon-helium plasma is reported and discussed in Sec. III. In Sec. IV, we shall review and adapt existing theories for the Mach number versus density perturbation and compare them with the experimental data.

II. EXPERIMENTAL CONDITIONS AND METHODS

The experiment was performed in a multipole double-plasma (DP) device.[13,14] To avoid any uncontrolled contamination of the plasma, the base pressure was kept as low as 2×10^{-7} Torr. In the case of the one-component plasma, the neutral gas pressure was $(1-2)\times10^{-4}$ Torr for Ar and $(8-9)\times10^{-4}$ Torr for He. With a total emission

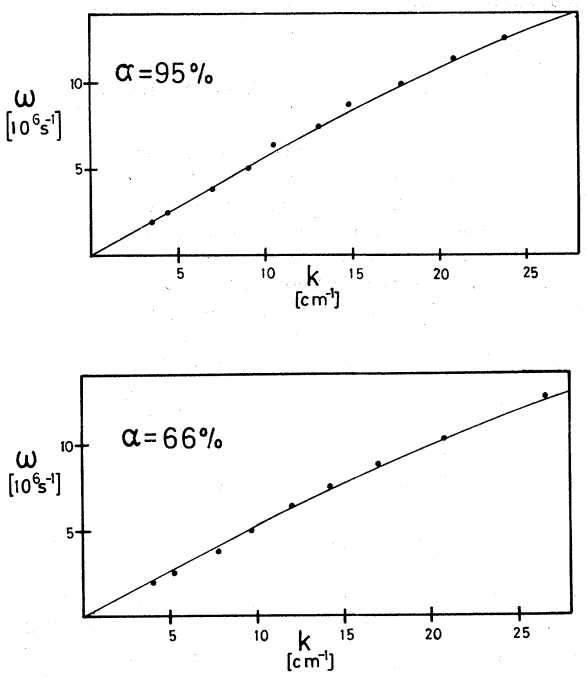

FIG. 1. Dispersion relation $\omega=\omega(k)$ of small-amplitude ion acoustic waves ($\delta_n/n_0 \sim 1\%$) for $\alpha=95\%$ and 66%. The value of λ_{De} is 0.028 cm and the values of different ion plasma frequencies, $\omega_{PiHe}=(\alpha n_0 e^2/\epsilon_0 M_{He})^{1/2}$ and $\omega_{PiAr}=[(1-\alpha)n_0 e^2/\epsilon_0 M_{Ar}]^{1/2}$, are, respectively, $1.74\times10^7\ s^{-1}$ and $1.26\times10^6\ s^{-1}$ for $\alpha=95\%$, and $1.45\times10^7\ s^{-1}$ and $3.29\times10^6\ s^{-1}$ for $\alpha=66\%$. The dispersion relations have also been measured for $\alpha=88\%$ and 76% and present the same qualitative features as the ones presented.

current of 400 mA, the plasma densities were 2×10^9 and $7\times10^8\ cm^{-3}$, respectively.

While working with the two-component plasma, the He and Ar neutral gases were introduced one after the other using two different inlets. This procedure provided us with an easy way of knowing the partial pressure of each gas. The total neutral pressure varies with the desired light-ion concentration α. However, the partial pressures of Ar and He were always kept below or equal to the values given previously. From the plasma density measured in pure He and Ar versus the respective neutral pressure dependence, α can be determined. We estimate the precision on the determination of α to be $\pm5\%$.

The electron temperature T_e and the electron-to-ion temperature ratio T_e/T_i were determined by measuring the complex wave vector, $k=k_r+ik_i$, of linear nondispersive ion acoustic waves. T_e was found to be about 1 eV and T_e/T_i around 9 ± 1. As reported previously,[12] in the presence of an Ar-He mixture, the electron and ion temperatures can be considered as constant, since the measured phase velocity and damping rate are well described by the solution of the dispersion relation computed with these values.

Since the soliton results from a delicate balance between nonlinearity and dispersion, it is therefore important to characterize the ion acoustic behavior of our plasma for dispersive waves. The dispersion relation of small-amplitude ion waves ($\delta n/n_0 < 1\%$) has been measured and is presented in Fig. 1 for $\alpha\sim95\%$ and 66%. The dots are from experiment, and the solid curve corresponds to the theoretical dispersion relation given by the root of

$$\mathcal{E}(\omega,k)=1+\frac{T_i}{T_e k^2}-\frac{1}{2k^2}\left[(1-\alpha)Z'\left(\frac{\omega}{k}\right)+\alpha Z'\left(\frac{\omega}{k}\mu^{-1/2}\right)\right]=0. \quad (2)$$

In Eq. (2), Z is the Fried-Conte function and μ the Ar-to-He mass ratio ($\mu=10$); the phase velocity ω/k is normalized to $(2T_i/M_{Ar})^{1/2}$ and k to $(n_0e^2/\epsilon_0T_i)^{1/2}$. The dispersion relation for an ion wave propagating in a pure Ar (or He) plasma has been reported elsewhere.[3] It has also been measured for other values of α for which solitons exist, namely, $\alpha=88\%$ and 76%. Aside from a variation of the phase velocity in agreement with the one given by Eq. (2), its shape is similar to the one given in Fig. 1. The $\omega=\omega(k)$ behavior does not differ much from the case of a pure plasma, since for these high values of α, the presence of Ar ions in a He plasma gives only an increase[12] of the effective ion mass[12] $M_{eff}=M_{Ar}/(1-\alpha+\alpha\mu)$. Solitons have been created by applying to the driver a positive, sinusoidal pulse with an amplitude up to 5 V and a pulse width of 5–12 μs. The resulting perturbation in the target plasma is detected by a flat Langmuir probe (5 mm diam) collecting electron saturation current. The signal is then monitored on an X-Y recorder using a boxcar-gated integrator (PAR 162). Greatest care has to be taken in the measurement of the soliton Mach number M (equal to the soliton velocity divided by the velocity of a linear perturbation C_s). Because C_s is sensitive to the presence of an ion beam in the plasma, the driver and target potentials have been carefully adjusted by comparing the wavelengths of linear ion waves propagating in both plasmas. The soliton velocity is deduced from measurements of the time of flight Δt between two neighboring positions x_0 and $x_0+\Delta x$. As a routine procedure, after each soliton measurement the propagation velocity of a linear pulse has also been measured in order to get C_s.

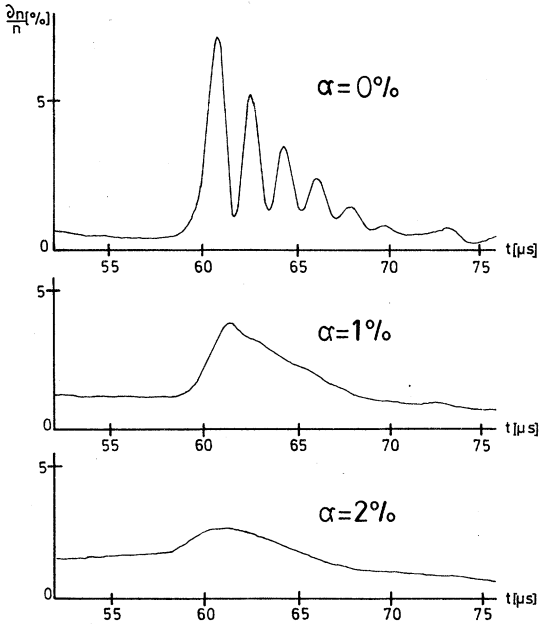

FIG. 2. Typical shapes of the nonlinear perturbation in the target plasma, 11 cm from the grid for small light-ion concentration α ($\alpha = 0\%$ corresponds to a pure Ar plasma).

III. EVOLUTION OF A NONLINEAR PULSE

The typical shape of the nonlinear pulse is given in the Figs. 2 and 3 for different light-ion concentrations at fixed distance. Figure 4 shows the steepening and the solition formation for a He-Ar plasma ($\alpha = 88\%$). For $\alpha = 0$ and 100%, the initial perturbation breaks into many solitons in spite of the relatively low temperature ratio, $T_e/T_i = 9$. Their properties (Mach number and width versus amplitude) have been reported elsewhere.[3] Their number also agrees with the number predicted by the Gardner *et al.*[15] inverse scattering method. As small amounts of the light ions are added to the Ar plasma, the structure suffers two main changes: first, a reduction in amplitude, and second, the disappearance of the solitons. With typical initial perturbations, no turbulence has been observed although the number of reflected ions was greatly increased. For higher α, the damping is high and the waves cannot propagate long enough to steepen.

The number of reflected ions also increases with α. In the lab frame, all ions of species j with a velocity between $MC_s - (2e\Phi_{max}/M_j)^{1/2}$ and MC_s will be reflected by the potential hill. For Ar ions, $MC_s \gg (2T_i/M_{Ar})^{1/2}$ so that the number of nonlinear resonant Ar particles is small. By contrast, $MC_s \simeq (2T_i/M_{He})^{1/2}$ and also $(2\Phi e_{max}/M_{He})^{1/2} \simeq (2T_i/M_{He})^{1/2}$ so that nearly all of the He ions which stream toward the potential hill will be reflected.

On the other side, the influence of Ar ions in a He plasma is much less pronounced. In Fig. 3, the perturbation structure is reported for high α. For $\alpha = 100\%$, the initial pulse also breaks into many solitons. However, their structure (Fig. 3, top) is different from the one in pure Ar (Fig. 2, top), although the important parameter, T_e/T_i, remains the same. In contrast to the case where $\alpha = 0\%$, the solitons are not well separated, and they appear as small peaks superimposed on the trailing edge of the pulse. No satisfactory explanation of this observation has been found. Up to $\alpha \simeq 66\%$, one still notices this separation into many peaks, although the smallest ones are less and less visible. Finally, for α below 66%, one gets only a smooth potential hump with no tendency towards separation into distinct peaks. In a previous work,[3] we identified each peak as a soliton, principally because their number corresponds to the one predicted by the inverse scattering method.[15] We can therefore state that we have solitons when the potential structure breaks into a few peaks. It is clear

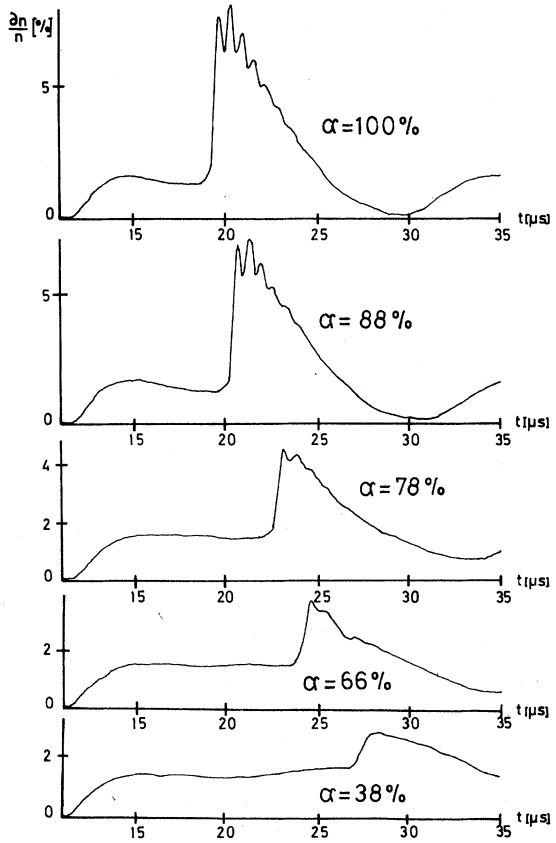

FIG. 3. Typical shapes of the nonlinear perturbation in the target plasma, 11 cm from the grid for high light-ion concentration α ($\alpha = 100\%$ corresponds to a pure He plasma).

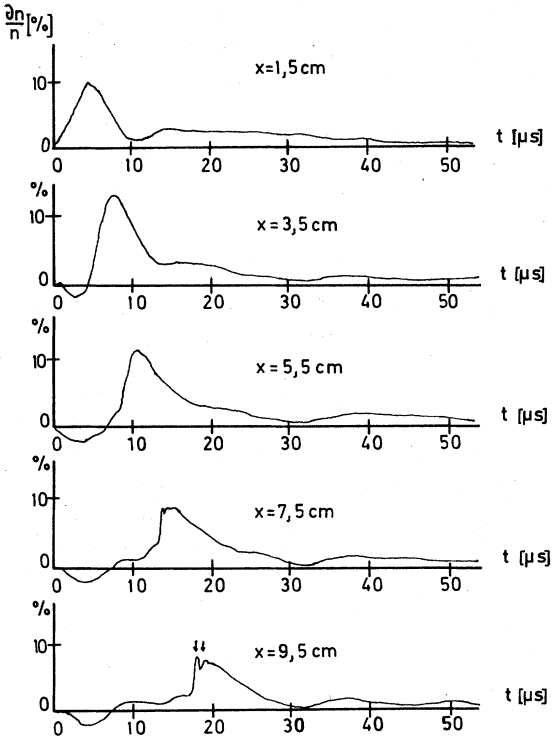

FIG. 4. Spatial evolution of the nonlinear perturbation for $\alpha = 88\%$. The arrows show the solitons. At $x = 0.5$ cm the amplitude of the perturbation is smaller than at 3.5 cm. This apparent contradiction is due to the direct pickup which is clearly seen in the other figure and which lowers down the amplitude of the measured signal. For longer distance, the perturbation amplitude damps down as expected.

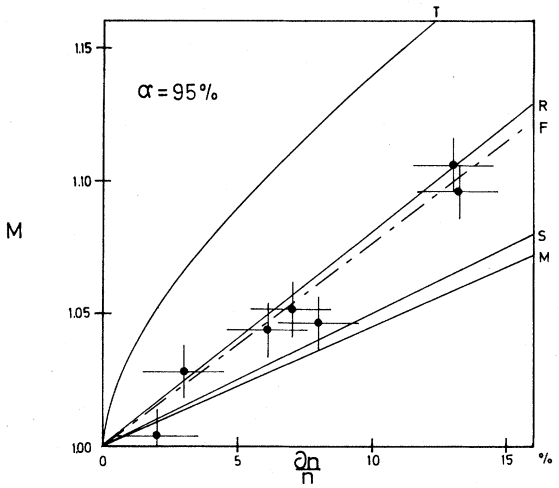

FIG. 5. Mach number versus density perturbation in a He-Ar plasma with $\alpha = 95\%$. (●, experiment; M, K-dV theory with $T_e/T_i = 9$; S, Sakanaka's theory; R, kinetic theory including reflected ions and trapped electrons; T, fluid theory including trapped electrons; F, best fit through the experimental points. The results from the K-dV equation with $T_i = 0$ are very close to the curve M and has not been drawn for clarity.)

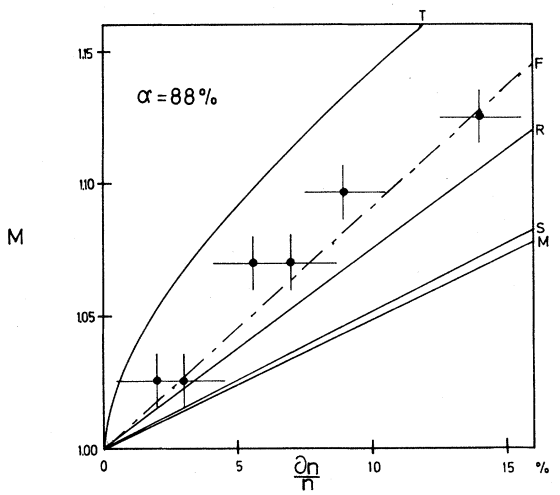

FIG. 6. Mach number versus density perturbation in a He-Ar plasma with $\alpha = 88\%$. Notations are similar to Fig. 5.

that in the case of a He-Ar mixture, their number cannot be counted precisely as in the case of a pure Ar or He plasma as the damping, which affects more the smallest solitons,[16] is increased, and only the highest solitons will be distinct. Using this statement, we conclude that solitons exist for $66\% < \alpha < 100\%$. Quantitative measurements of the Mach number M and width D/λ_{De} versus the amplitude $\delta n/n_0$ of the first peak confirm their soliton character (Figs. 5–9). The Mach number M increases and D/λ_{De} decreases with $\delta n/n_0$. The M vs $(\delta n/n_0)$ dependences will be discussed in more detail in Sec. IV.

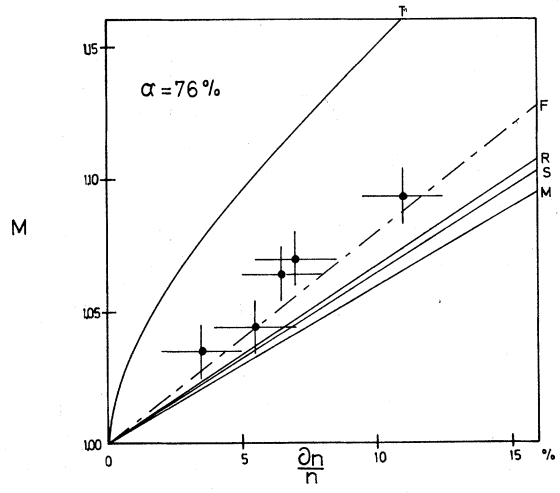

FIG. 7. Mach number versus density perturbation in a He-Ar plasma with $\alpha = 76\%$. Notations are similar to Fig. 5.

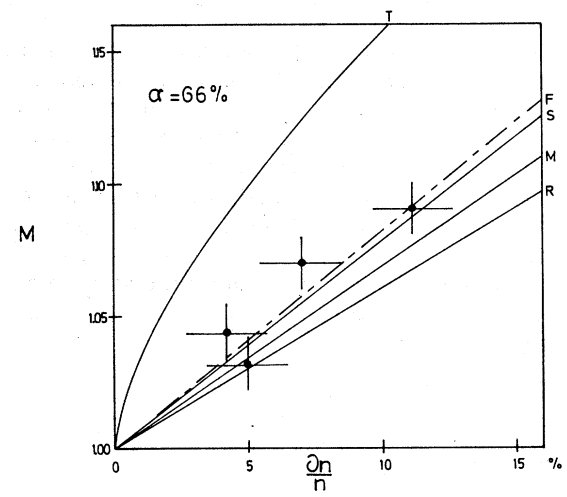

FIG. 8. Mach number versus density perturbation in a He-Ar plasma with $\alpha = 66\%$. Notations are similar to Fig. 5.

The spatial evolution of a nonlinear pulse perturbation in a two-ion species also exhibits some interesting features. For a pure Ar plasma, the perturbation amplitudes decay near the middle grid and then, as the first soliton is forming, the amplitude of the first peak starts increasing before decreasing again because of Landau damping (Fig. 10). Adding a small amount of He ($\alpha \sim 1\%$), the perturbation no longer increases its amplitude as before but continuously damps out. The damping rate is near the one observed with a linear pulse ($\delta n/n_0 \sim 1\%$). The amplitude reduction observed between $\alpha = 0\%$ and $\alpha = 1\%$ (Fig. 3) can be simply attributed to linear damping and not to any nonlinear effect due to the presence of light ions as predicted by the K-dV equation.[5,6] In the case of pure He, or in a mixture of He and Ar ($\alpha < 66\%$), the perturbation continuously damps out as it propagates away from the grid as can be seen in Fig. 11.

IV. MACH NUMBER VERSUS SOLITON AMPLITUDE DEPENDENCE

The experimental data are reported in Figs. 5–12 for different concentrations. As expected from nonlinear phenomena, the Mach number increases linearly with $\delta n/n_0$. We shall now examine the variation rate of M versus $\delta n/n_0$ using different theories.

A. Korteweg-de Vries equation for a two-ion-species plasma ($T_i = 0$)

In this model,[5] the plasma is described by fluid equations for both ion species, assuming $T_i = 0$. The electrons obey Boltzmann's law. Finite but small electron perturbations $\delta n/n_0$ are then described by the following K-dV equation:

$$2\frac{\partial}{\partial \eta}\left(\frac{\delta n}{n_0}\right) + A\left(\frac{\delta n}{n_0}\right)\frac{\partial}{\partial \xi}\left(\frac{\delta n}{n_0}\right) + \frac{\partial^3}{\partial \xi^3}\left(\frac{\delta n}{n_0}\right) = 0 , \tag{3}$$

where

$$A = \frac{3(\mu^2\alpha + 1 - \alpha)}{(1 - \alpha + \alpha\mu)^2} - 1 ,$$

and ξ and η are the usual stretched coordinates ($\xi = x - t$, $\eta = x$). The relationship between Mach number and $\delta n/n_0$ is therefore

$$\frac{\delta n}{n_0} = \frac{6(M-1)}{3(\mu^2\alpha + 1 - \alpha)/(1 - \alpha + \alpha\mu)^2 - 1} . \tag{4}$$

It is instructive to compare the experimental ratio $(\delta n/n_0)/(M-1)$ to the theoretical one (Fig. 12). The experimental value of $(\delta n/n_0)/(M-1)$ has been determined by a least-squares fitting of the measured values. The discrepancy between the predictions from the K-dV equation and the experimental points is obvious: the K-dV formalism predicts an increase of $(\delta n/n_0)/(M-1)$ with α, whereas one observes experimentally that this quantity is roughly constant.

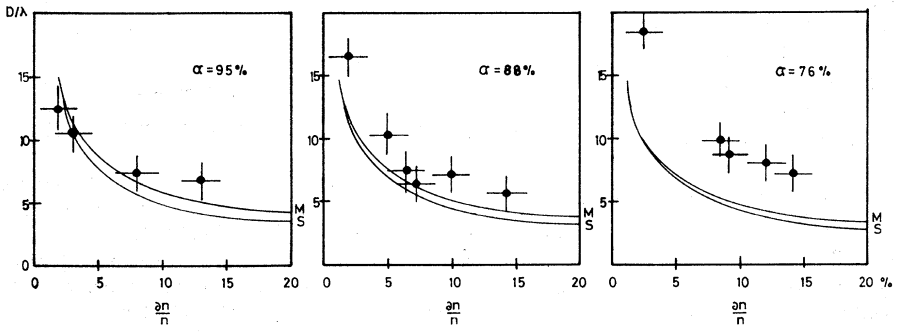

FIG. 9. Width of the soliton as a function of its amplitude for different light-ion concentrations (●, experiment; M, K-dV theory with $T_i \neq 0$; S, Sakanaka's theory).

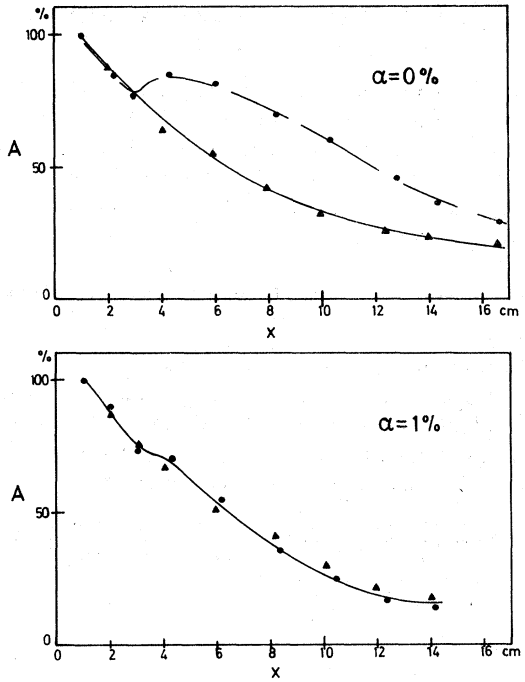

FIG. 10. Spatial evolution of the amplitude of a soliton (●) and a linear perturbation ($\delta n/n_0 \sim 1\%$) (▲) for a pure Ar plasma and for $\alpha = 1\%$. The amplitude reported has been normalized to its value at $x = 1$ cm from the grid. The nonlinear perturbation amplitude $\delta n/n_0$ at $x = 1$ cm is 18% for $\alpha = 0\%$ and 1%. The decrease in amplitude of the soliton in the latter case ($\alpha = 1\%$), which becomes apparent at $x = 4$ cm, is then mainly due to linear damping.

Since in our plasma the ratio T_e/T_i is rather low ($T_e/T_i = 9$), one would expect better agreement with the experimental data if T_i is taken into account. In the following, we shall discuss two fluid models which include the ion temperature T_i in their equations, and finally a stationary Vlasov formalism.

B. Korteweg-de Vries equation for a two-ion-species plasma ($T_i \neq 0$)

The plasma is modeled by fluid equations for the two-ion species with an adiabatic equation of state for the ions ($p_i = T_i n_i^3$). The adiabatic law for ions is a reasonable one since the phase velocity ω/k is greater than both ion thermal velocities. The electron density is assumed to be Boltzmann-like. Using a reductive method, the evolution of the nonlinear disturbance is described by a K-dV equation whose coefficients are complicated functions of T_e/T_i and α.[6]

In Figs. 5–8 and 12, the M vs $\delta n/n_0$ and $(\delta n/n_0)/(M-1)$ dependencies are reported.[18] One finds only a slight change from the above results (Fig. 12) and therefore this model seems inadequate to explain our experimental results.

C. Sakanaka's model

Originally, Sakanaka[18] only treated the case of a one-component plasma. The basic equations are the well-known fluid equations for ions. The ion temperature is also considered via an adiabatic pressure law. The electrons are assumed to be Boltzmann-like and the whole set equation is closed by Poisson's equation. Instead of using a perturbation method as before, one studies directly the stationary solution of the fluid equations.[17] In a frame moving at velocity V, Poisson's equation then reduces to

$$\frac{\partial^2 \Phi}{\partial x^2} = e^{\Phi} - \sum_{j=1}^{2} n_j = -\frac{dU}{d\Phi}, \tag{5}$$

with

$$n_j = \left(\frac{\alpha_j^2}{6\theta\mu_j}\right)^{1/2} \{V^2 + 3\theta\mu_j - 2\mu_j\Phi - [(V^2 + 3\theta\mu_j - 2\mu_j\Phi)^2 - 12V^2\mu_j\theta]^{1/2}\}^{1/2}. \tag{6}$$

In Eqs. (5) and (6), the density is normalized to the unperturbed electron density n_0, velocity to

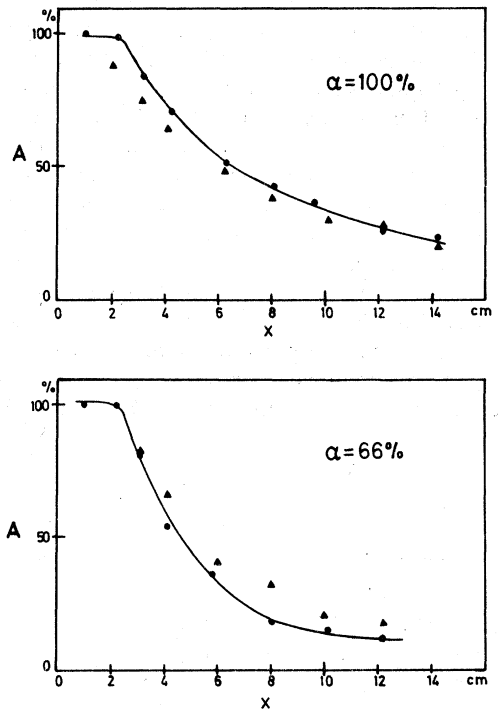

FIG. 11. Spatial evolution of the amplitude of a soliton (●) and a linear perturbation (▲) for $\alpha = 100\%$ and 66%. $\delta n/n_0$ at $x = 1$ cm is equal to 12.3% and 11.1% for $\alpha = 100\%$ and 66%, respectively. Note the increase in linear Landau damping for $\alpha = 66\%$, which corresponds to that expected from the linear dispersion relation.

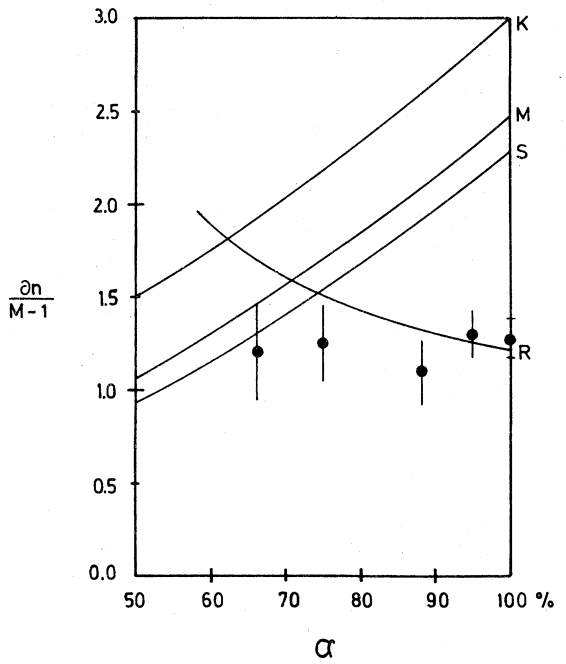

FIG. 12. Variation of the normalized soliton amplitude $(\delta n/n_0)/(M-1)$ with the concentration α. Curves K and M correspond respectively to results from the K-dV equation with $T_i=0$ and $T_e/T_i=9$. Curve S shows the result from Sakanaka's theory; R, from kinetic theory including reflected ions and trapped electrons. ● represents experimental values using linear regression.

$(T_e/M_{Ar})^{1/2}$, Φ to T_e/e, and distance to $(\epsilon_0 T_e/n_0 e^2)^{1/2}$; $\theta=T_i/T_e$, and

$$\alpha_j=\begin{cases}\alpha, & j=1\\ 1-\alpha, & j=2\end{cases};\quad \mu_j=\begin{cases}\mu, & j=1\\ 1, & j=2\end{cases}.$$

The pseudopotential $U(\Phi)$ is then given by

$$U(\Phi)=1-e^{\Phi}+\sum_{j=1}^{2}\int_0^{\Phi} n_j(\varphi)\,d\varphi.$$

It is then obvious that $U(\Phi=0)=0$. Stationary solution then exists if $U(\Phi)<0$. The soliton amplitude Φ_{max} for a given V is the first nonzero solution of the equation

$$U(\Phi)=0. \tag{7}$$

Numerical solutions of (7) have been computed for different V and used to trace the different curves of Figs. 5–8. The Mach number M is defined as V/λ with[6]

$$\lambda^2=(1-\alpha+\alpha\mu)+\frac{3\theta(1-\alpha+\alpha\mu^2)}{1-\alpha+\alpha\mu},$$

which corresponds to the velocity of an infinitesimally small stationary structure. Although the numerical values given by this model are closer to the experimental data than the above ones, its α dependency is similar to the one given by the different K-dV equations: $(\delta n/n_0)/(M-1)$ always increases with α, leaving a discrepancy between theory and experiment.

D. Kinetic model

All the previous models do not take into account the reflected ions. In a one-species plasma their number, and consequently their influence, can be neglected. (In Watanabe's experiment[19] even no precursor of reflected ions has been observed!) As mentioned in Sec. II, their number increases when a second ion species is introduced. It is therefore necessary to study their influence in the propagation characteristic of a nonlinear structure. Before going into detail, one should point out that, basically, a model which takes into account reflected ions admits as a stationary solution only shock[20] and not solitons. However, one would expect that the Mach number versus $\delta n/n_0$ dependence is not affected, and hence the result may be used to fit our experimental data. The formalism used is analogous to the one used by White *et al.*[4] We have extended their theory by using a Vlasov equation for Ar ions and by introducing a maximally trapped equation of state for electrons[21]:

$$\frac{\delta n}{n_0}=2(\Phi/\pi)^{1/2}+e^{\Phi}\operatorname{erfc}(\Phi^{1/2}). \tag{8}$$

This equation of state was used mainly for two reasons. For our temperature ratio $T_e/T_i=9$, using a Boltzmann-type equation of state, $n_e=n_0e^{\Phi}$, one would not expect any stationary solution even in a one-component plasma. Following Bardotti and Segre,[22] stationary structure does not exist if $T_e/T_i>12.35$. But the principle reason is that low-energy electrons are actually trapped in the potential well of the solitons. Evidence of trapped electrons in a large-amplitude ion wave propagating in an unstable plasma has been published by Wong *et al.*[23] In a more recent article, Tran and Means[24] reported on the observation of a flat-topped electron distribution measured in the positive large-amplitude ($e\Phi/T_e\gtrsim 5\%$) potential perturbation (sinusoidal as well as soliton structure) of a stable plasma. These measurements allow us to state that low-energy electrons are trapped in the soliton well and, consequently, the use of Eq. (8) to describe the electron equation of state is much more adequate than the usual Boltzmann one.

Equation (8), combined with fluid equations for ions ($T_i=0$), gives the following pseudopotential $U(\Phi)$:

$$U(\Phi)=1-P+\sum_{j=1}^{2}\frac{\alpha_j V}{\mu_j}\left[V-(V^2-2\Phi\mu_j)^{1/2}\right], \tag{9}$$

where

$$P = 2(\Phi/\pi)^{1/2} + e^{\Phi}\,\mathrm{erfc}(\Phi^{1/2}) + 4\Phi^{3/2}/3\pi^{1/2}. \qquad (10)$$

The M vs $\delta n/n_0$ dependence is reported in Figs. 5–8. The experimental point now lies well below the theoretical work. It is therefore not sufficient to consider only trapped electrons and fluid equations for ions.

Using now the same kinetic formalism as White *et al.*,[4] we get the following expression for the pseudopotential:

$$-U(\Phi) = \Big(1 + \sum_j \alpha_j r_j\Big)[P(\Phi) - P(0)] + \sum_j \alpha_j A_j \mu_j^{-1} (2\pi\theta\mu_j)^{-1/2} \Big[\int_{(2\Phi\mu_j)^{1/2}}^{\infty} dv\, W_j(v,\Phi) + \int_{(2\Phi\mu_j)^{1/2}}^{(2\Phi_m\mu_j)^{1/2}} dv\, W_j(v,\Phi) - \int_0^{\infty} dv\, W_j(v,0) - \int_0^{(2\Phi_m\mu_j)^{1/2}} dv\, W_j(v,0)\Big], \qquad (11)$$

with the definitions

$$A_j = \frac{2}{1 + \mathrm{erf}[V/(2\theta\mu_j)^{1/2}]},$$

$$r_j = \tfrac{1}{2} A_j \{\mathrm{erf}[V/(2\theta\mu_j)^{1/2}] + \mathrm{erf}[(\Phi_m/\theta)^{1/2} - V/(2\theta\mu_j)^{1/2}]\}, \qquad (12)$$

$$W_j(v,\Phi) = v(v^2 - 2\Phi\mu_j)^{1/2} \exp\{-(v - V^2)^2/2\theta\mu_j\}.$$

The first and second integrals represent the contributions of incident and reflected ions, respectively. The third and fourth integrals are integration constants which ensure that $U(\Phi = 0) = 0$.

In this model, we define the Mach number M as the ratio of V to the velocity obtained for a small stationary perturbation ($\delta n/n_0 < 0.5\%$). The results are in better agreement with the experimental data as shown in Fig. 12. One also notes the interesting dependence of $(\delta n/n_0)/(M-1)$ vs α: In contrast to other models, where this quantity increases with α, it predicts a slight decrease of this quantity when α tends to 1. This feature is not surprising since an analogous property is also found in a one-component plasma as T_e/T_i increases. Numerical computations of Means *et al.*[25] show an increase in amplitude of a shock at a given M number when T_e/T_i decreases. In both cases (i.e., when α or T_e/T_i increases), the number of reflected ions decreases and less energy is taken away from the structure. In the experimental uncertainty, this feature agrees with the observed variation (Fig. 12). The model also gives the number of reflected ions for different α. For the α range, where solitons are observed, the number of reflected ions are mainly He ions since the soliton velocity is closer to the He thermal velocity than the Ar one. The experimental data are in close agreement with the theory (Figs. 13 and 14). For $\alpha \sim 1\%$, one notes an increase in reflected He ions: As expected, nearly all of the He ions with a velocity towards the potential structure are reflected. Such an increase is also consistent with our measurement.

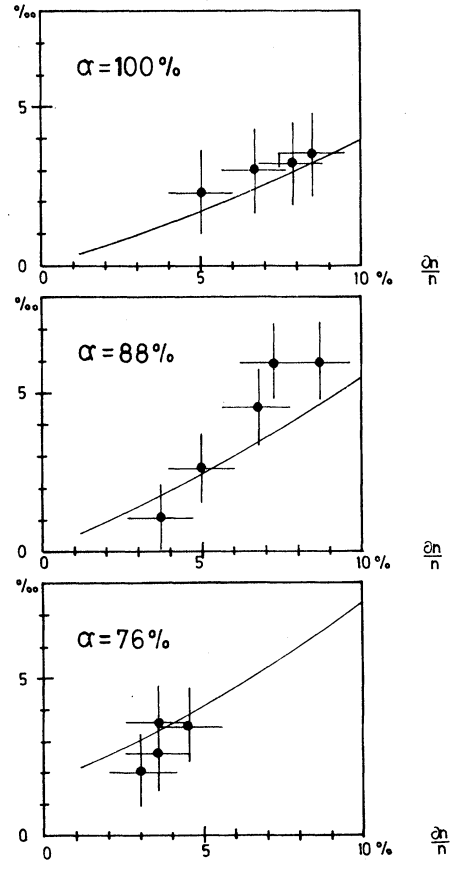

FIG. 13. Number of reflected ions, R, versus the soliton amplitude $\delta n/n_0$ ($\alpha = 100\%$, 88%, and 76%). ● represents experimental points. The curve was deduced from formulas (12).

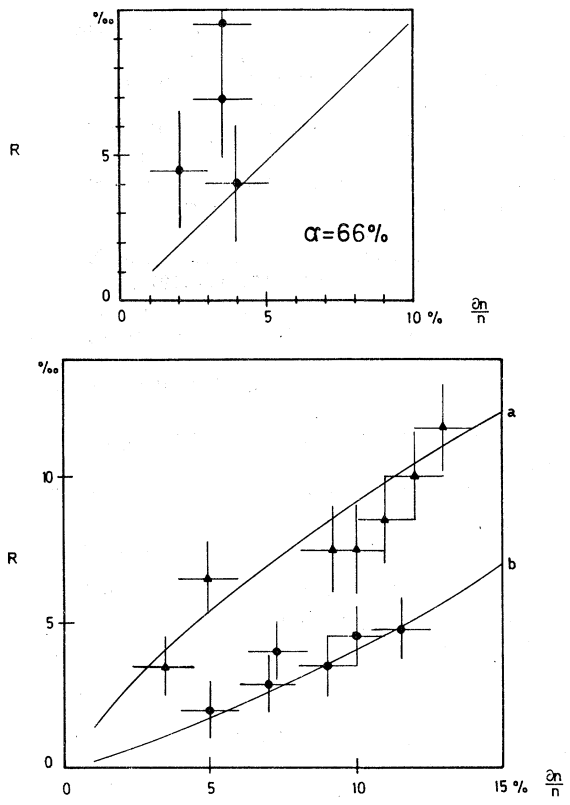

FIG. 14. Number of reflected ions, R, versus the soliton amplitude $\delta n/n_0$ for $\alpha = 66\%$, 1%, and 0%. ▲ and curve (a) correspond to $\alpha = 1\%$; ● and curve (b), to $\alpha = 0\%$.

V. DISCUSSION AND CONCLUSION

Our experimental study allows the following statements:

(a) In a heavy-ion plasma, light-ion contamination ($\alpha \sim 1\%$) inhibits the formation of ion acoustic solitons.

(b) The influence of heavy ions in a light-ion plasma is less pronounced. A concentration of nearly 40% of heavy ions can be added without destroying completely the soliton structure.

(c) In the latter case, the properties of the structure are adequately described by a kinetic theory which takes into account the reflected ions. The agreement between the kinetic theory and experiment also brings an answer to the question of relative importance between kinetic and hydrodynamic effects: It is clearly shown that no fluid theory does fit well with experimental data.

Our experiment also suggest that, for $\alpha > 1\%$, the dominant cause which inhibits the soliton formation is reflected and trapped ions, and not Landau damping. From Fig. 12, the e folding in the amplitude of a perturbation is nearly the same in a plasma without any light-ion contamination as in one with a small amount of He ions; in the second case, however, the number of reflected ions is drastically increased. Although no measurement of trapped ions in the potential hill formed between two neighboring solitons has been performed, the following ordering of the bounce frequencies Ω_{Bj} of the different ion species gives some insight to the role of the light ion in preventing soliton formation. Normalizing Ω_{Bj} (j = Ar, He) to $\Omega_{P\mathrm{Ar}}$ and distance to λ_{De}, we have

$$\Omega_{B\mathrm{Ar}} = \Phi^{1/2} 2\pi/\lambda_s\,, \quad \Omega_{B\mathrm{He}} = (10\Phi)^{1/2} 2\pi/\lambda_s\,,$$

and the ion Landau damping frequency Ω_i is then given by

$$\Omega_i = 2\pi\omega_i/(\omega_r \lambda_r)\,.$$

λ_s is the separation between two neighboring solitons; λ_r measures the rising slope of the soliton ($\lambda_r \sim$ soliton width). For the case reported in Fig. 3 we have the following ordering:

$$\Omega_i = 4\times10^{2}, \quad \Omega_{B\mathrm{Ar}} = 7\times10^{-2}, \quad \Omega_{B\mathrm{He}} = 21\times10^{-2},$$

and

$$\Omega_i \lesssim \Omega_{B\mathrm{Ar}} < \Omega_{B\mathrm{He}}\,.$$

As the values of both Ω_i and $\Omega_{B\mathrm{Ar}}$ are similar to the one in the case of a pure-Ar plasma (a 1% light-ion concentration does not change appreciably either the density or the damping, as can be seen in Fig. 12) where solitons exist, it appears, as a consequence of our ordering, that effects due to trapped ions are more important than Landau damping.

For the high-α range ($66\% \lesssim \alpha < 100\%$), it is more difficult to determine, aside from ion reflection, whether damping of the trapped-particle effect is dominant. Since we are dealing now with a plasma containing mainly He, one should normalize all of the frequencies to $\Omega_{P\mathrm{He}}$. We have now, for $60\% \lesssim \alpha < 100\%$:

$$4\times10^{-2} < \Omega_i < 8\times10^{-2}, \quad \Omega_{B\mathrm{He}} \approx 7\times10^{-2}.$$

From this ordering, it is reasonable to state that both effects are now important.

ACKNOWLEDGMENT

It is a pleasure to acknowledge fruitful discussions with Dr. M. Bitter, Dr. D. Grésillon, Dr. R. W. Means, Dr. J. Vaclavik, and Professor E. S. Weibel. The technical assistance of H. Ripper and his team was appreciable. This work has been performed under the auspices of the Fonds National Suisse pour la Recherche Scientifique.

[1]H. Ikezi, R. J. Raylor, and D. R. Baker, Phys. Rev. Lett. 25, 11 (1970).
[2]H. Ikezi, Phys. Fluids 16, 1668 (1973).
[3]Ch. Hollenstein and M. Q. Tran, Helv. Phys. Acta 49, 547 (1976). Some misprints have been found in this paper. An Erratum appeared in Helv. Phys. Acta 50, 283 (1977).
[4]R. B. White, B. D. Fried, and F. V. Coroniti, Phys. Fluids 15, 1484 (1972).
[5]M. Q. Tran and P. J. Hirt, Plasma Phys. 16, 617 (1974).
[6]M. Q. Tran, Plasma Phys. 16, 1167 (1974).
[7]S. Maxon, Phys. Fluids 19, 266 (1976).
[8]E. Ott and R. N. Sudan, Phys. Fluids 12, 2388 (1969).
[9]Y. Kato, M. Tajiri, and T. Taniuti, Phys. Fluids 15, 865 (1972).
[10]J. W. van Dam and T. Taniuti, J. Phys. Soc. Jpn. 35, 897 (1973).
[11]B. D. Fried, R. B. White, and Th. K. Samec, Phys. Fluids 14, 2388 (1971).
[12]M. Q. Tran and S. Coquerand, Phys. Rev. A 14, 2301 (1976).
[13]R. Limpaecher and H. R. McKenzie, Rev. Sci. Instrum. 44, 726 (1973).
[14]P. J. Hirt and M. Q. Tran, Helv. Phys. Acta 47, 473 (1972).
[15]C. S. Gardner, J. M. Greene, M. D. Kruskal, and R. S. Miura, Phys. Rev. Lett. 19, 1095 (1957).
[16]N. Hershkowitz, T. Romesser, and D. Montgomery, Phys. Rev. Lett. 29, 1586 (1972).
[17]In Ref. 6 the author normalized the velocity to $(T_e/M_{Ar})^{1/2}$. In order to compare the theoretical value with the experimental data, where velocity is normalized to the actual ion sound velocity, the following formula should be taken for $(\delta n/n_0)/(M-1)$: $(\delta n/n_0)/(M-1)=3/P$, instead of $3/\lambda P$ as given in Ref. 6.
[18]P. N. Sakanaka, Phys. Fluids 15, 304 (1972).
[19]S. Watanabe, J. Plasma Phys. 14, 353 (1975).
[20]S. S. Moiseev and R. Z. Sagdeev, J. Nucl. Energy C 5, 43 (1967).
[21]D. W. Forshund and C. R. Shonk, Phys. Rev. Lett. 25, 1699 (1970).
[22]G. Bardotti and S. E. Segre, Plasma Phys. 12, 247 (1970).
[23]A. Y. Wong, B. H. Quon, and B. M. Ripin, Phys. Rev. Lett. 30, 1299 (1973).
[24]M. Q. Tran and R. W. Means, Phys. Lett. 59A, 128 (1976).
[25]R. W. Means, F. V. Coroniti, A. Y. Wong, and R. B. White, Phys. Fluids 16, 2304 (1973).